Impact of physical-chemistry on the film thinning in surface bubbles

Marina Pasquet, François Boulogne, Julien Sant-Anna, Frédéric Restagno, Emmanuelle Rio

Impact of physical-chemistry on the film thinning in surface bubbles

Marina Pasquet[1], François Boulogne[1], Julien Sant-Anna[1], Frédéric Restagno[1], and Emmanuelle Rio[1]

[1]Laboratoire de Physique des Solides, CNRS, Univ. Paris-Sud, Université Paris-Saclay, Orsay 91405, France

July 6, 2022

Abstract

In this paper, we investigate the thinning dynamics of evaporating surfactant-stabilised surface bubbles by considering the role of the physical-chemistry of solutions used in the liquid bath. We study the impact of the surfactant concentration below and above the cmc (critical micelle concentration) and the role of ambient humidity. First, in a humidity-saturated atmosphere, we show that if the initial thickness depends on the surfactant concentration and is limited by the surface elasticity, the drainage dynamics are very well described from the capillary and gravity contributions. These dynamics are independent of the surfactant concentration. In a second part, our study reveals that the physical-chemistry impacts the thinning dynamics through evaporation. We include in the model the additional contribution due to evaporation, which shows a good description of the experimental data below the cmc. Above the cmc, although this model is unsatisfactory at short times, the dynamics at long times is correctly rendered and we establish that the increase of the surfactant concentration decreases the impact of evaporation. Finally, the addition of a hygroscopic compound, glycerol, can be also rationalized by our model. We demonstrate that glycerol decreases the bubble thinning rate at ambient humidity, thus increasing their stability.

1 Introduction

The study of surface bubbles have raised a large research interest due to the broad range of applications. For instance, we can cite industrial applications such as the flavor of fizzy drinks [1], or the understanding of the dispersion of pollutants above swimming pools [2]. In addition, understanding the bubble bursting phenomenon is crucial for modelling the climate, as the process is involved in the quantification of the gas exchange between the ocean and the atmosphere [3, 4].

In presence of surfactants, the bubble lifetime is primarily fixed by the thinning velocity [5], which in turn is due to two mechanisms, the drainage, and the liquid evaporation. Indeed, the film surrounding surface bubbles has been proven to thin down to a few tens of nanometers, the thickness at which bursting occurs. To understand and to be able to predict the lifetime of these bubbles, it is therefore necessary to consider their thinning dynamics [6].

In absence of evaporation, the drainage is driven by the competing effects of capillary suction [7] and gravity [5]. This process is limited by the flow through a pinch developing at the bottom of the surface bubbles, in the vicinity of the meniscus [8]. Such a description has been verified experimentally, either in a saturated atmosphere, *i.e.* in absence of evaporation [5] or at a short time, when evaporation is negligible over the drainage [7, 9].

Nevertheless, evaporation must be taken into account for thicknesses typically lower than one micrometer [10]. To describe the thinning rate in presence of evaporation, a constant evaporation rate can be added to the mass conservation. Such consideration provides a successful description of the data available in the literature [9, 5].

A noticeable consequence of this description lies on the role of the liquid composition, which is expected to modify the thinning process, and thus the bubble lifetime, only through the liquid viscosity, density, and surface tension. This observation conflicts to the common intuition and daily observations that the choice of the soapy solution recipe is fundamental to control bubbles stability [11], whereas viscosity, density, and surface tension are slightly modified.

Hence, the aim of the paper is to identify the role of physical-chemistry on surface bubble thinning, and in particular to precise separately the specific effects on drainage and on evaporation. To make this distinction, we performed experiments in a saturated atmosphere to identify the role of the surfactant concentration on thinning dynamics, without any evaporation phenomena. Then, additional experiments are presented in an atmosphere controlled in humidity to investigate the role of evaporation.

system	c	γ (mN/m)	ρ (kg/m^3)	η (mPa·s)
TTAB	0.5 cmc	50.2	998	1.00
TTAB	1 cmc	38.2	998	1.00
TTAB	5 cmc	35.9	998	1.00
TTAB	10 cmc	35.7	998	1.00
TTAB	20 cmc	35.2	998	1.00
TTAB/Gly	0.5 cmc	42.3	1047	1.74
TTAB/Gly	20 cmc	23.4	1047	1.74

Table 1: Surface tension γ measured for TTAB solutions at different concentrations noted c in the table, at 20 °C (at ± 0.2 mN/m). TTAB used for the solutions at 0.5 and 1 times the cmc have been recrystallized. The denomination "TTAB/Gly" corresponds to solutions containing a mass concentration of glycerol of 20 %.

2 Experimental setup

2.1 Material

In this study, we use TTAB (Tetradecyl Ammonium Bromide, purchased from Sigma-Aldrich) as well as glycerol (purity ≤ 99.5 % purchased from VWR) diluted in ultrapure water (resistivity = 18.2 MΩ·cm). The TTAB solutions are prepared for several concentrations between 0.5 and 20 times the critical micelar concentration (cmc = 3.6 mmol·L^{-1}). Since impurities in surfactant solutions have a noticeable effect on surface properties below the cmc, TTAB used 0.5 and 1 times the cmc is recrystallized prior to the preparation of the solutions [12].

To investigate the impact of glycerol on the stability of surface bubbles, solutions with TTAB are made by replacing ultrapure water with a mixture of ultrapure water and glycerol with an initial glycerol concentration $c_{g_0} = 20$ wt%.

The surface tensions γ of our solutions are measured with a pendant drop commercial apparatus (Tracker, Teclis) and the results are reported in Table 1. The viscosity η and the density ρ of the solutions containing TTAB in water are assumed to be identical to the pure water properties. The viscosity and density of solution containing glycerol are estimated from data on water-glycerol mixtures available in the literature [13, 14].

2.2 Bubble generation and thinning measurement

The experimental setup is schematized in Fig. 1. Bubbles are generated on the surface of a cylindrical Plexiglas tank of 4.0 cm diameter and 4.6 cm depth, filled with a solution up to the rim. To inject air in the solution, a PTFE tubing with an external diameter of 0.56 mm (from Cole-Parmer) is inserted at the base of the tank. This extremity of the tube is beveled and placed just below the surface of the solution. To circumvent the flexibility of the PTFE tubing, the later is inserted
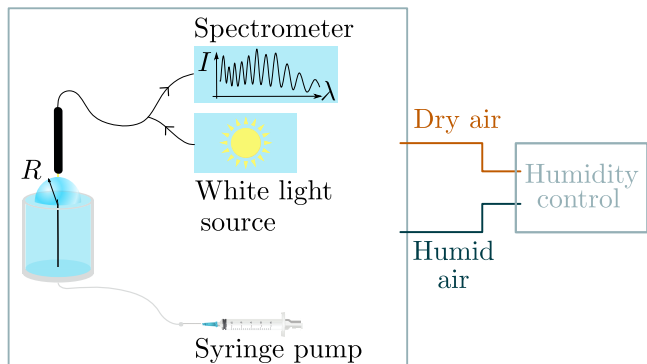

Figure 1: A container with the solution of interest is set in a humidity-controlled chamber. To generate the bubble, air is injected by a syringe pump. The film thickness at the apex of the surface bubble is measured by white light spectrometry.

in a glass capillary tube. The opposite extremity of the PTFE tubing is then connected to a flexible tube of 6 mm diameter, and about 80 cm long connected to a 50 mL syringe. The syringe is placed on a syringe pump (AL-1000 from WPI), such that the airflow rate Q and the injected volume Ω_{air} are perfectly controlled. In this study, we choose to keep the injected volume $\Omega_{\text{air}} = 1.50$ mL constant, as it has already been varied in a previous study [5]. The the flow rate $Q = 15$ mL·min^{-1} is also kept constant, such that the bubble radius of curvature $R = 1.03 \pm 0.08$ cm is also constant.

The temperature is monitored and ranges between 20 and 23 °C. The whole device is enclosed in a chamber of size $40 \times 40 \times 50$ cm^3. The humidity is controlled through a humidity regulator [15]. For experiments conducted at 100 % humidity, a humidifier (Bionaire BU1300W-I) and wet towels are also used to saturate the box with water vapor.

The thickness h of the film at the apex of the bubble cap is measured using a UV-VIS spectrometer (Ocean Optics Nanocalc 2000), whose wavelengths are between 450 and 800 nm, associated with a 200 μm diameter optical fiber. The spectrometer must be positioned vertically, precisely at the apex to allow the spectrometer to be perpendicular to the film. The tank containing the solution is thus placed on a xy-translation plate. The thickness is extracted from the spectrum of the reflected light using the *Oospectro* [16] library written in Python [5, 17]. The temporal evolution of the film thickness is measured two or three times for each experimental condition. As the measurements are perfectly reproducible, the results presented will correspond systematically to two or three repetitions of the same experiment condition and for better readability, the symbols will be the same. The initial time ($t = 0$) corresponds to the end of the bubble generation.

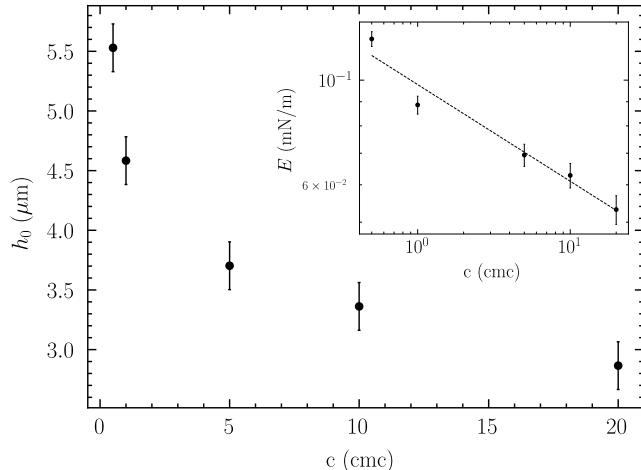# 3 Impact of physical-chemistry on thin film drainage

Figure 2: Variation of the initial thickness of surfactant solutions as a function of the TTAB concentration. The error bars correspond to the estimated accuracy of 0.2 μm on the determination of the initial thickness. The inset shows the Gibbs-Marangoni elasticity of the film obtained from h_0 using Eq. 1. The dashed line is a power law fit: $E = 0.10 \, c^{-0.20}$. The initial thicknesses plotted correspond to those obtained by leaving h_0 as an adjustable parameter when we compare Eq. 2 to our data, shown in Fig. 3.

3.1 Initial thickness

In this Section, we consider the experiments performed in a saturated atmosphere, so that we expect the thinning to be due solely to drainage since no evaporation occurs. Once the bubble is inflated at the surface of the surfactant solution, after the 6 seconds of generation, the thickness of the bubbles at the apex is referred to as the initial thickness and is noted h_0. The measurements of h_0 extracted from our drainage curves are presented in Fig. 2, which shows a decrease of the initial thickness with the surfactant concentration.

To understand the variation of h_0 with the surfactant concentration, a first approach is to adopt the description of the film generation based on a Frankel-type mechanism [18]. In this model, the thickness is set by a balance between the capillary suction in the meniscus and the viscous dissipation in the thin film, characterized by the capillary number $Ca = \eta V / \gamma$ with the entrainment velocity V. The Frankel description leads to an initial thickness $h_0 \sim \ell_c \, Ca^{2/3}$, where $\ell_c = \sqrt{\gamma/(\rho g)}$ is the capillary length, with g the gravitational acceleration.

In the present study, all bubbles are generated with the same flow rate, $i.e.$ the same entrainment velocity V.

Additionally, the surfactant concentration affects mainly the surface tension γ (table 1). The difference of surface tension between TTAB at 0.5 and 20 cmc is of 15 mN/m. This leads to a difference of 0.4 μm for h_0, much lower than what is measured. As a consequence, this model predicts a nearly identical initial thicknesses for all bubbles based on Frankel's mechanism. This prediction is in contradiction with the observations presented in Fig. 2. In previous experiments, performed at similar injection rates, the initial thickness of surface bubbles was shown to be rather independent on the flow rate [10].

Therefore, we conclude that the soap film generation is not driven by a viscous flow, but rather by elasticity [19, 20]. In an elasticity-dominated regime, the thickness is limited by the surface elasticity E, $i.e.$ by the ability of the surface to sustain surface concentration gradients and thus surface tension gradients.

In this regime, the balance between the capillary suction and the Marangoni stress due to surfactant surface concentration inhomogeneities at the interfaces leads to a thickness independent on the generation velocity [19, 20]:

$$h_0 \sim \ell_c \frac{E}{\gamma}. \tag{1}$$

With this prediction, the initial thickness is expected to depend on the surfactant concentration through the surface elasticity E. Here, we propose to apply the same model to the surface bubbles, although there is likely so existing refinements from the geometry and deduce the surface elasticity from the initial thickness measurements and comment the result. The accordance with the experiments performed on flat films show that this model still holds for surface bubbles. From our data $h_0(c)$ and Eq. 1, we plot in the inset of Fig. 2 the predicted surface elasticity. We obtain a decay of the surface elasticity with the surfactant concentration, which we describe with a power law model. Such decrease is expected since a larger surfactant concentration allows a faster repopulation of the interfaces and thus a smaller surface elasticity [21]. The measurement of surface elasticity is delicate and rare in the literature. In our study, the order of magnitude of the surface elasticity is 0.1 mN/m, which is lower but in agreement with those measured by Champougny $et\ al.$ [19] ($C_{12}E_6$), which are between 0.15 and 0.59 mN/m. This non-ionic surfactant is much less soluble that TTAB. In such a situation, the surface elasticity is expected to be slightly higher, in agreement with our experiment. In the literature, one can also find higher values [22, 23, 24, 25] for the surface elasiticity. Nevertheless, a direct comparison can be hazardous since this parameter is expected to depend drastically on the physical-chemistry and on the characteristic time of solicitation. Our observation is that the values measured here are comparable to surface elastic moduli measured with similar systems and a similar solicitation.
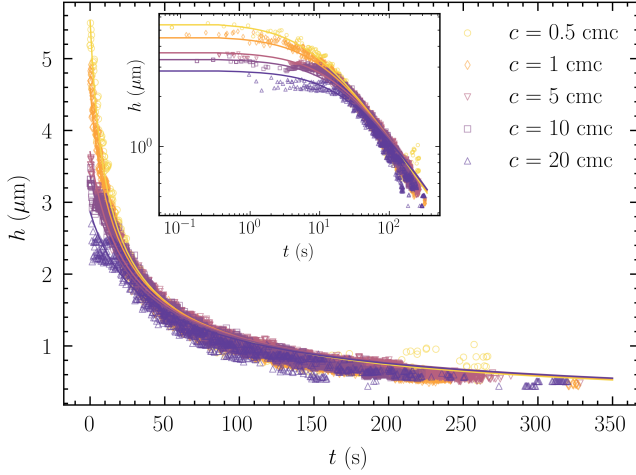
Figure 3: Film drainage in a saturated environment for bubbles stabilized by different concentrations of TTAB ranging in 0.5-20 cmc. The continuous lines correspond to Eq. 2. The same graph is represented in inset in logarithmic scale.

3.2 Thinning dynamics

Now that the initial thickness is described, we focus our attention on the thinning dynamics. All the drainage curves obtained for the different TTAB concentrations are presented in Fig. 3. Remarkably, the thinning process appears to be nearly independent on the surfactant concentration, besides the initial thickness described in the previous paragraph.

In the following, we compare these thinning dynamics with the drainage model described in the introduction, in which the flow is limited by the presence of a pinch in the vicinity of the contact line [7, 9, 5]. The thinning rate is therefore the combination of capillary-driven and gravity-driven flows, which reads [5]

$$\frac{\partial h}{\partial t} \ = \ - \ \frac{\gamma}{\eta} \left(\frac{h^{5/2}}{R^{5/2}} + \frac{h^3}{R\ell_c^2} \right), \qquad (2)$$

Indeed, the gravity-driven drainage is relevant in our situation because the Bond numbers Bo comparing the effect of gravity and surface tension (Bo $= \rho g R^2 / \gamma$) corresponding to our bubbles are between 20 and 44. To solve this differential equation we used the odeint function from the scipy module [26] in Python. The initial thickness of the bubbles h_0 is left as an adjustable parameter for the integration of Eq. 2, *via* the use of the curve_fit function of the scipy module [26]. This thickness is plotted as a function of TTAB concentration in Fig. 2. We have chosen to leave it as an adjustable parameter in order to be able to describe the long time dynamics of all our systems in the presence of evaporation, as we will see later. Fig. 3 shows that the experimental data agree with this theoretical prediction (solid lines). Note that an implicit solution to the Eq. 2 can be de-

termined analytically. The calculation and the result are given in S.I.

Finally, our first conclusion is that, in absence of evaporation, the concentration in TTAB does not impact the drainage dynamics. This is confirmed by the results of Poulain *et al* [9] for bubbles of radius $R = 4.8 \pm 0.1$ mm with another surfactant, SDS (Sodium Dodecyl Sulfate). The only impact of the physical-chemistry is a short-time effect. The liquid composition changes the initial thickness through the variation of the surface elasticity. After a few tens of seconds, which is short compared to the bubble draining time, all the dynamics becomes independent of the TTAB concentration. We thus expect a negligible impact on the bubble lifetime.

4 Impact of physical-chemistry on thin film evaporation

4.1 Control of evaporation via the atmospheric humidity

To explore the impact of physical-chemistry on evaporation, we now measure the thinning dynamics at relative humidity values RH equal to 39 and 55 %.

As expected, the dynamics is much faster in presence of evaporation so that the bubble lifetime is more than 5 times shorter. Additionally, in conditions for which evaporation proceeds, the thinning dynamics for different surfactant concentrations do not collapse in a single curve as shown in Fig. 4. This observation contrasts with the results in a saturated atmosphere obtained in the previous Section. Thus, although the surfactant concentrations studied in this article have a little impact on the drainage dynamics, this concentration affect significantly the thinning of the bubbles when evaporation proceeds.

To describe the thinning dynamics, we add an evaporation rate[9, 5] to the former drainage Eq. 2. For this, we can consider a diffusive evaporation rate [27], which is proportional to the difference in pressure between the saturation vapour pressure at the interface p_{sat} and in the surrounding environment p_∞. We write the contribution of the evaporation on the film thinning as $k_e(1 - \text{RH})$, where k_e has the dimension of a velocity. This coefficient contains the geometry of the system, kept constant in this study, the diffusion coefficient of water in air, and the saturated vapor pressure of the chemical solution. This leads to the thinning rate

$$\frac{\partial h}{\partial t} \ = \ - \ \frac{\gamma}{\eta} \left(\frac{h^{5/2}}{R^{5/2}} + \frac{h^3}{R\ell_c^2} \right) \ - \ k_e \left(1 - \text{RH} \right). \qquad (3)$$

The model describes very well the data for TTAB concentration smaller or equal to the cmc for both RH $= 39$ and 55 %. For the solutions containing TTAB above the cmc, the proposed model does not allow to account
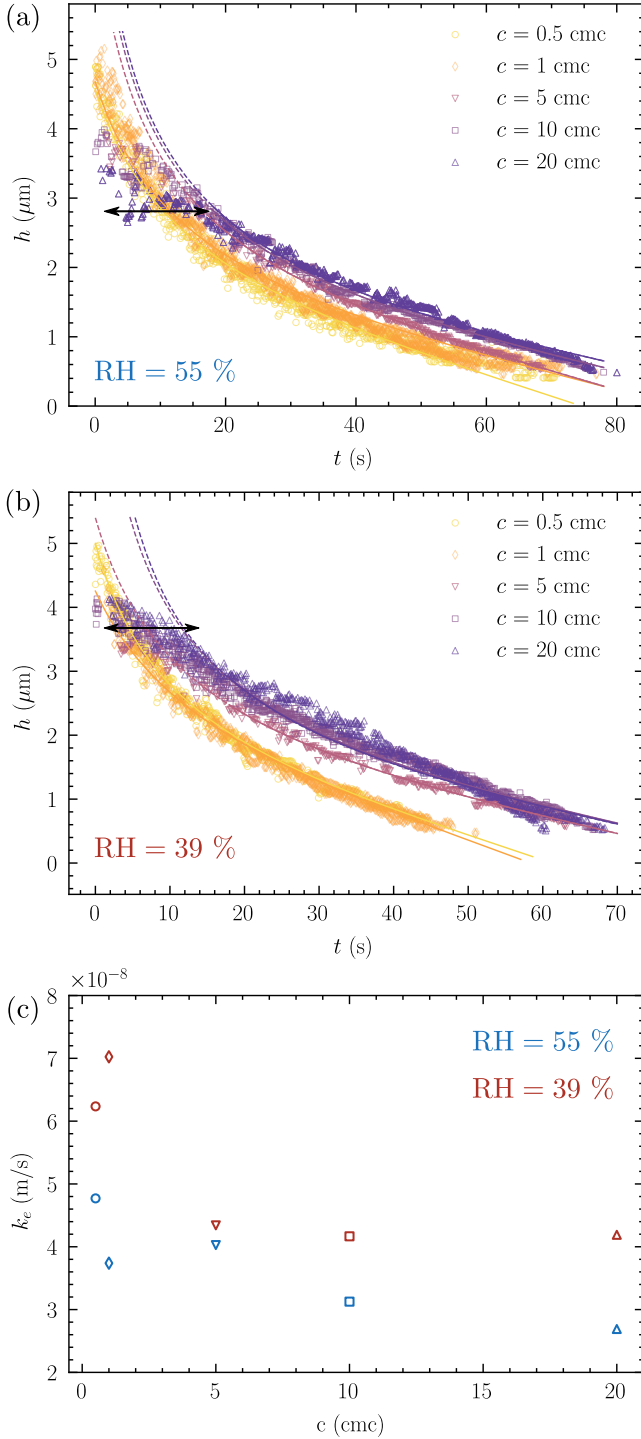
(a)

h (μm)

$c = 0.5$ cmc
$c = 1$ cmc
$c = 5$ cmc
$c = 10$ cmc
$c = 20$ cmc

RH = 55 %

t (s)

(b)

h (μm)

$c = 0.5$ cmc
$c = 1$ cmc
$c = 5$ cmc
$c = 10$ cmc
$c = 20$ cmc

RH = 39 %

t (s)

(c)

$\times 10^{-8}$

k_e (m/s)

RH = 55 %
RH = 39 %

c (cmc)

Figure 4: Film thinning at the bubble apex in a environment of controlled humidity of (a) $RH = 55 \pm 4$ % and (b) $RH = 39 \pm 1$ %, for bubbles stabilized by different concentrations of TTAB ranging in 0.5-20 cmc. The continuous lines correspond to Eq. 3 using k_e (given in (c)) as a fitting parameter. For c > cmc, the fit was made from $t = 18$ s: the extrapolation to the first instants is indicated by a dotted line.

for the beginning of the thinning curves. We observe that, in presence of evaporation, the thinning dynamic is delayed at the beginning for these concentrations, especially for the highest concentration (20 times the cmc) where a plateau, marked by a black arrow, can be observed. Thus, a fit for these "high" concentrations is proposed only at times greater than 18 seconds (Fig. 4 (a) and (b)). In this case, there is a good agreement between our model and the experimental data. It can be noted that for concentrations above cmc, the higher the TTAB concentration, the slower the evaporative thinning dynamics, as indicated by the measured k_e constant values given in the Fig. 4 (c).

Our second result is thus that the variation of the TTAB concentration affects the thinning dynamics of surface bubbles through the evaporation rate. A simple model, in which a constant evaporation flux is added to the drainage dynamics allows describing the data in the first order. This is actually a simple model, which cannot capture the entire thinning dynamics. Indeed, at high concentration, the variation of h with time is poorly described by our model. Our strong result is that the physical chemistry affects the thinning dynamics mainly through evaporation and not through drainage. Similar behaviour has already been observed by Poulain *et al.*[2]. Nevertheless, the exact mechanism behind this observation will deserve more investigation in the future: capturing the evaporation mechanisms in a single parameter, which is the evaporation rate is actually a simplified model. Indeed evaporation can also lead to temperature gradients, surfactant bulk and surface concentration gradients, which can lead to Marangoni stresses at the interface and affect the thinning dynamics.

4.2 Control of evaporation *via* the addition of an hygroscopic component

In the following, the surface bubbles studied are generated at RH = 55 $\pm$ 5 % in water-glycerol mixtures for two concentrations of the TTAB solution (equal to 0.5 and 20 times the cmc).

The thinning curves obtained for bubbles stabilized by TTAB/glycerol/water solutions, with an initial glycerol concentration $c_{g_0} = 20$ wt.%, are plotted in Fig. 5. Comparing these results to those obtained with TTAB/water only, we can see that the addition of glycerol stabilizes the bubbles by decreasing their thinning rate at long times (in particular for the concentration corresponding to 20 times the cmc). We also note that the bursting thickness is still high, around 1.5 μm in Fig. 5 (a). It has been demonstrated that the lifetime can have a wide distribution since the mechanism behind is partially stochastic [7]. Thus, this is not necessarily a robust feature that the bubbles burst at such high thickness but the thinning dynamics holds in any case.

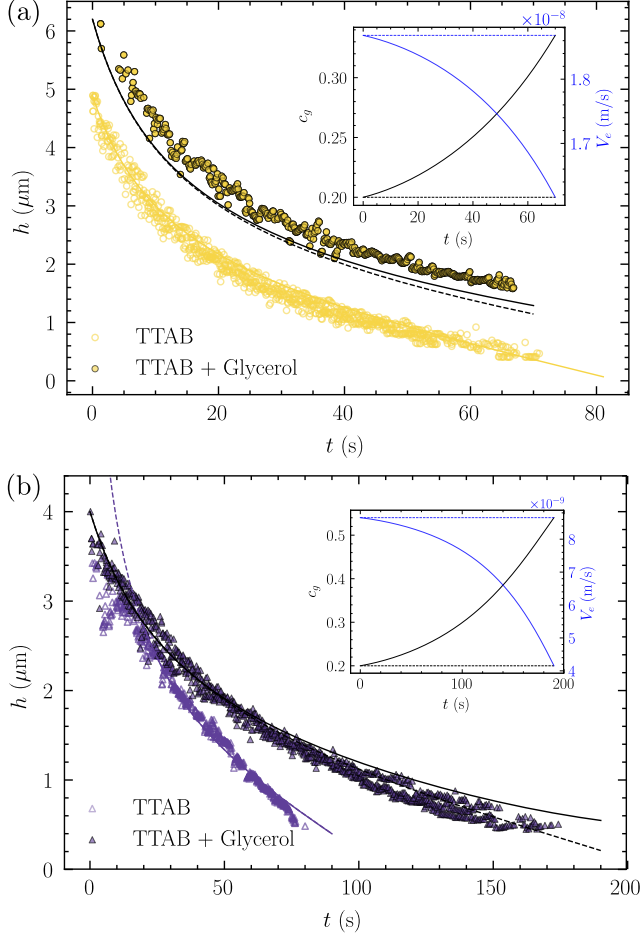To rationalize this observation, we propose to take into

Figure 5: Time evolution of the film thickness h at the bubble apex in a environment of controlled humidity $(55 \pm 5\%)$ for bubbles stabilised with or without an initial glycerol concentration $c_{g_0} = 20$ wt.%, for fixed TTAB concentrations: (a) 0.5 cmc and (b) 20 cmc. The data in the absence of glycerol and the corresponding colour adjustment correspond to those shown in Fig. 4. For the data in the presence of glycerol, the black dotted line corresponds to the Eq. 5 with a constant concentration $c_g = c_{g_0}$. The black solid line corresponds to this equation taking into account the variation of c_g with time, by combining Eq. 6, 7 and 5. The inset shows the variation of c_g and V_e for these two cases.

account the addition of glycerol in the thinning dynamics. Glycerol is a hygroscopic component, known to affect the solution activity[28] and thus, its evaporation rate [29, 30]. The saturation vapour pressure $p_{\mathrm{sat}}(c_g)$ at the evaporating interface is modified by the presence of glycerol in the solution and can be written as [29]:

$$p_{\mathrm{sat}}(c_g) = p_{\mathrm{sat}}(c_g = 0)\frac{1 - c_g}{1 + c_g(a - 1)} \quad (4)$$

with $a = 0.248$ [31, 29].

As in Eq. 2, the drainage caused by the capillary suction and gravity remains unchanged. Only the evaporation term is modified by taking into account the change in saturation vapour pressure at the interface given by Eq. 4, which leads to writing the thinning rate such as

$$\frac{\partial h}{\partial t} = -\frac{\gamma}{\eta}\left(\frac{h^{5/2}}{R^{5/2}} + \frac{h^3}{R\ell_c^2}\right) - k_e\left(\frac{1 - c_g}{1 + c_g(a - 1)} - \mathrm{RH}\right). \quad (5)$$

The thinning rate corresponding to evaporation, the second term on the right hand side of this equation, can therefore be positive or negative, which means that in the presence of glycerol, the water can either evaporate (positive term) or condense (negative term). This depends on both the glycerol concentration and the relative humidity.

In this section, we will not consider any adjustable parameter to integrate the Eq. 5: the initial thickness h_0 corresponds to the experimentally measured value and the evaporation constant k_e to the value determined in the previous paragraph, in the absence of glycerol. The prediction of Eq. 5, for a constant glycerol concentration $c_g(t) = c_{g_0}$, is shown in black dotted lines in Fig. 5.

However, the mass concentration c_g varies over time and we can attempt to quantify this effect. To integrate Eq. 5, the time evolution of the glycerol concentration $c_g(t)$ must be precised from the exchanges with the bath and the atmosphere. We consider that the bubble has a spherical cap of volume $\Omega(t) = 2/3\pi(3R^2h(t) + 3Rh(t) + h(t)^3)$, for which the liquid composition is homogeneous. The weight of glycerol in the bubble is defined as $m_g(t) = c_g(t)\rho\Omega(t)$. From the definition of the glycerol concentration $c_g(t) = m_g(t)/(m_g(t) + m_w(t))$, we have $m_w(t) = (1 - c_g(t))\rho\Omega(t)$. The time variation of the glycerol weight in the spherical cap is due to drainage of velocity $V_d[h(t)] = \gamma/\eta\left(h^{5/2}/R^{5/2} + h^3/(R\ell_c^2)\right)$, which gives

$$\frac{\mathrm{d}m_g}{\mathrm{d}t} = -\rho_g V_d[h(t)]S\Phi_g(t), \quad (6)$$

where $S = 2\pi R^2$ is the surface area of the hemispherical cap and $\Phi_g(t) = (1 + \rho_g/\rho_w(1/c_g(t) - 1))^{-1}$ is the volume concentration of glycerol. Similarly, for the water content, the variations is due to the drainage velocity V_d but also the evaporation velocity $V_e[c_g(t)] =$

$k_e\left((1 - c_g)/(1 + c_g(a - 1)) - \mathrm{RH}\right)$, such that

$$\frac{\mathrm{d}m_w}{\mathrm{d}t} = -\rho_w V_d[h(t)]S\Phi_g(t) - \rho_w V_e[c_g(t)]S. \quad (7)$$

We solve equations 5, 6 and 7 for the following initial conditions, using an Euler-type method: $c_{g_0} = 0.2$, $m_{w0} = (1 - c_{g_0})\rho\Omega_0$ and $m_{g0} = c_{g_0}\rho\Omega_0$ with $\Omega_0 = 2/3\pi(3R^2h_0 + 3Rh_0 + h_0^3)$ the volume of the liquid in the bubble cap at $t = 0$. Note that the measured surface tension of water/glycerol mixtures in presence of TTAB remains almost constant up to $c_g = 0.4$, so we used the value given in the Tab. 1.

The results of this integration are shown in Fig. 5 with black solid lines, describing relatively well the temporal evolution of the measured thickness for the two concentrations. They show a weak effect, to first order, of taking into account the variation of c_g with time. The inset shows the evolution of the glycerol concentration and the evaporation rate during the thinning of the bubbles. As time goes by, the glycerol concentration increases, which leads to a decrease in the evaporation rate and therefore the bubble thinning rate. We attribute the enhanced stability of these bubbles at longer times to the reduction of the thinning rate.

5 Conclusion

In absence of evaporation, physical-chemistry has no impact on the thinning dynamics of surface bubbles. It affects only the initial thickness, which can be explained by a surface elasticity depending on the surfactant concentration. In presence of evaporation, the thinning dynamics is affected by the TTAB concentration. This effect can be explained at the first order by an evaporation flux depending on the TTAB concentration. Nevertheless, a more precise description of this dynamic probably requires a better understanding of the role of surfactants on evaporation. This role can be due to a barrier exerted by the surfactants to evaporation [32], which could explain the variation of the evaporation rate with the surfactant concentration. Evaporation could also generate additional solutal or thermal surface tension gradients, which could add a stabilizing or destabilizing liquid flow [9, 33]. Additionally, the water evaporation could lead to a variation of the local concentration in surfactants, which can also affect the flow and/or evaporation rate. This work thus opens new questions, which shall be answered in a future work and will benefit from the exploration of a wider range of chemical systems. Furthermore, we observed that the addition of glycerol slows down the thinning dynamics. Even if we know that numerous potential mechanisms at stake due to evaporation in presence of surfactants or surfactants/glycerol solutions can occur [34, 35, 36], the simple model presented in this article allows a good description of the data. The effect of the addition of glycerol can be described by considering both the modification of the saturation vapor pressure in the presence of glycerol and the increasing glycerol concentration in time due to water evaporation.

We have enlightened that the description of surface bubbles thinning dynamics requires a better understanding of the effect of physical-chemistry on evaporation. This effect can come from different mechanisms (i) the concentration of non volatile components along time [31] (ii) the existence of a barrier to evaporation due to the presence of surfactants at the interface, which can affect the evaporation flux [32] or the apparition of solutal or thermal surface tension gradient [9, 33], which can lead to additional liquid velocities.

Acknowledgments

References

[1] Gérard Liger-Belair, Clara Cilindre, Régis D. Gougeon, Marianna Lucio, Istvan Gebefügi, Philippe Jeandet, and Philippe Schmitt-Kopplin. Unraveling different chemical fingerprints between a champagne wine and its aerosols. *Proceedings of the National Academy of Sciences*, 106(39):16545–16549, 2009.

[2] S. Poulain and L. Bourouiba. Biosurfactants change the thinning of contaminated bubbles at bacteria-laden water interfaces. *Phys. Rev. Lett.*, 121:204502, Nov 2018.

[3] DM Murphy, JR Anderson, PK Quinn, LM McInnes, FJ Brechtel, SM Kreidenweis, AM Middlebrook, Mihaly Pósfai, DS Thomson, and PR Buseck. Influence of sea-salt on aerosol radiative properties in the southern ocean marine boundary layer. *Nature*, 392(6671):62–65, 1998.

[4] Olivier Boucher, David Randall, Paulo Artaxo, Christopher Bretherton, Gragam Feingold, Piers Forster, V-M Kerminen, Yutaka Kondo, Hong Liao, Ulrike Lohmann, et al. Clouds and aerosols. In *Climate change 2013: the physical science basis. Contribution of Working Group I to the Fifth Assessment Report of the Intergovernmental Panel on Climate Change*, pages 571–657. Cambridge University Press, 2013.

[5] Jonas Miguet, Marina Pasquet, Florence Rouyer, Yuan Fang, and Emmanuelle Rio. Stability of big

surface bubbles: impact of evaporation and bubble size. *Soft Matter*, 16(4):1082–1090, 2020.

[6] Jonas Miguet, Florence Rouyer, and Emmanuelle Rio. The life of a surface bubble. *Molecules*, 26(5):1317, 2021.

[7] Henri Lhuissier and Emmanuel Villermaux. Bursting bubble aerosols. *Journal of Fluid Mechanics*, 696:5–44, 2012.

[8] A Aradian, E Raphaël, and P.-G. de Gennes. Marginal pinching in soap film. *Europhys. Lett.*, 55(6):834–840, 2001.

[9] S Poulain, E Villermaux, and L Bourouiba. Ageing and burst of surface bubbles. *Journal of fluid mechanics*, 851:636–671, 2018.

[10] Lorène Champougny, Matthieu Roché, Wiebke Drenckhan, and Emmanuelle Rio. Life and death of not so bare bubbles. *Soft matter*, 12(24):5276–5284, 2016.

[11] Stephen Frazier, Xinyi Jiang, and Justin C Burton. How to make a giant bubble. *Physical Review Fluids*, 5(1):013304, 2020.

[12] Cosima Stubenrauch and Khristo Khristov. Foams and foam films stabilized by cntab: influence of the chain length and of impurities. *Journal of colloid and interface science*, 286(2):710–718, 2005.

[13] Nian-Sheng Cheng. Formula for the viscosity of a glycerol- water mixture. *Industrial & engineering chemistry research*, 47(9):3285–3288, 2008.

[14] Andreas Volk and Christian J Kähler. Density model for aqueous glycerol solutions. *Experiments in Fluids*, 59(5):1–4, 2018.

[15] F. Boulogne. Cheap and versatile humidity regulator for environmentally controlled experiments. *The European Physical Journal E*, 42(4):51, 2019.

[16] François Boulogne. Oospectro: Get thicknesses from ocean optics spectra, 2019–.

[17] Jonas Miguet, Marina Pasquet, Florence Rouyer, Yuan Fang, and Emmanuelle Rio. Marginal regeneration-induced drainage of surface bubbles. *Phys. Rev. Fluids*, 6:L101601, Oct 2021.

[18] K Shinoda J. Mysels S. Frankel. *Soap Films: studies of their thinning*. Pergamon Press, New York - London - Paris - Los Angeles, 1959.

[19] Lorène Champougny, Benoit Scheid, Frédéric Restagno, Jan Vermant, and Emmanuelle Rio. Surfactant-induced rigidity of interfaces: a unified approach to free and dip-coated films. *Soft matter*, 11(14):2758–2770, 2015.

[20] Jacopo Seiwert, Benjamin Dollet, and Isabelle Cantat. Theoretical study of the generation of soap films: role of interfacial visco-elasticity. *Journal of fluid mechanics*, 739:124–142, 2014.

[21] Dominique Langevin. Rheology of adsorbed surfactant monolayers at fluid surfaces. *Annual review of fluid mechanics*, 46:47–65, 2014.

[22] Y. Couder, J.M. Chomaz, and M. Rabaud. On the hydrodynamics of soap films. *Physica D: Nonlinear Phenomena*, 37(1):384–405, 1989.

[23] A Prins, C Arcuri, and M van den Tempel. Elasticity of thin liquid films. *Journal of Colloid and Interface Science*, 24(1):84–90, 1967.

[24] Ildoo Kim and Shreyas Mandre. Marangoni elasticity of flowing soap films. *Phys. Rev. Fluids*, 2:082001, Aug 2017.

[25] A. Prins and M. Van den Tempel. Composition and elasticity of thin liquid films. *The Journal of Physical Chemistry*, 73(9):2828–2834, 1969.

[26] E. Jones, T. Oliphant, P. Peterson, et al. SciPy: Open source scientific tools for Python, 2001–.

[27] N A Fuchs. *Evaporation and droplet growth in gaseous media*. Pergamon Press, 1959.

[28] A. Bouchaudy, C. Loussert, and J.-B. Salmon. Steady microfluidic measurements of mutual diffusion coefficients of liquid binary mixtures. *AIChE Journal*, 64(1):358–366, 2018.

[29] Glycerine Producers' Association et al. *Physical properties of glycerine and its solutions*. Glycerine Producers' Association, 1963.

[30] Cong Chen, Wei Zhong Li, Yong Chen Song, and Jian Yang. Hydrogen bonding analysis of glycerol aqueous solutions: a molecular dynamics simulation study. *Journal of Molecular Liquids*, 146(1-2):23–28, 2009.

[31] Aymeric Roux, Alexis Duchesne, and Michael Baudoin. Everlasting bubbles and liquid films resisting drainage, evaporation, and nuclei-induced bursting. *Phys. Rev. Fluids*, 7:L011601, Jan 2022.

[32] Victor K La Mer. *Retardation of evaporation by monolayers: transport processes*. Academic Press, 2014.

[33] Xueliang Li, Ryan Shaw, and Paul Stevenson. Effect of humidity on dynamic foam stability. *International Journal of Mineral Processing*, 94(1-2):14–19, 2010.

[34] Yaxing Li, Christian Diddens, Pengyu Lv, Herman Wijshoff, Michel Versluis, and Detlef Lohse. Gravitational effect in evaporating binary microdroplets. *Phys. Rev. Lett.*, 122:114501, Mar 2019.

[35] Sangwoo Shin, Ian Jacobi, and Howard A. Stone. Bénard-Marangoni instability driven by moisture absorption. *EPL (Europhysics Letters)*, 113(2):24002, January 2016.

[36] Quentin Magdelaine-Guillot de Suduiraut. *Hydrodynamique des films liquides hétérogènes*. PhD thesis, Sorbonne Université, 2019.